Molecular Crystals and Liquid Crystals

Publication details, including instructions for authors and subscription information:
http://www.tandfonline.com/loi/gmcl20

Langmuir-Blodgett Film of Amphiphilic 8-Aminoquinoline and its Sensitivity to Copper Ion

Jian-Ming Ouyang [a]

[a] Institute of Biomineralization and Lithiasis Research, Jinan University, Guangzhou China, and State Key Laboratory of Materials Chemistry and Applications of Peking University, Beijing, China

Version of record first published: 31 Aug 2006

To cite this article: Jian-Ming Ouyang (2005): Langmuir-Blodgett Film of Amphiphilic 8-Aminoquinoline and its Sensitivity to Copper Ion, Molecular Crystals and Liquid Crystals, 428:1, 111-125

To link to this article: http://dx.doi.org/10.1080/154214090892753

Mol. Cryst. Liq. Cryst., Vol. 428, pp. 111–125, 2005

ISSN: 1542-1406 print/1563-5287 online
DOI: 10.1080/154214090892753

Taylor & Francis
Taylor & Francis Group

Langmuir–Blodgett Film of Amphiphilic 8-Aminoquinoline and its Sensitivity to Copper Ion

Jian-Ming Ouyang
Institute of Biomineralization and Lithiasis Research, Jinan University, Guangzhou China, and State Key Laboratory of Materials Chemistry and Applications of Peking University, Beijing, China

Two amphiphilic bis-amide tetradenate ligands based on 8-aminoquinoline, N,N′-bis(8-quinolinyl)alkylpropanediamide (H_2A) [alkyl: dodecyl (H_2A^{12}) and hexadecyl (H_2A^{16})], were synthesized and characterized by Fourier transform infrared (FT-IR) ^{1}H-Nuclear magnetic resonance (^{1}H NMR), and Ultraviolet-visible (UV-vis) spectroscopy. H_2A can form stable monolayers. The interactions between the H_2A monolayer and metal ions such as the main group of metallic ions (Mg^{2+}, Ca^{2+}, Pb^{2+}) and transitional metallic ions (Mn^{2+}, Co^{2+}, Ni^{2+}, Cu^{2+}, Zn^{2+}, Cd^{2+}, Hg^{2+}, and La^{3+}) were investigated. Only the Cu^{2+} ion has special coordination with H_2A monolayers. This coordination has been clearly proved by means of the π-A isotherms, X-ray photoelectron spectroscopy, and UV-vis spectroscopy. The selective copper binder of the Langmuir–Blodgett (LB) film of H_2A may be developed as a sensor of copper ion. H_2A^{16} LB film can detect the concentration of Cu(II) ion in the region of $1.0 \times 10^{-7} \sim 1.0 \times 10^{-6}$ mol dm^{-3}.

Keywords: 8-aminoquinoline; copper ion; Langmuir–Blodgett film; sensor

INTRODUCTION

Sensing supramolecules for s-block and d-block metal ions were developed in the past decade [1,2]. A bis-amide tetradentate ligand derived from 8-aminoquinoline has been developed as a photo-induced electron-transfer sensor for transition metal ions in our laboratory [3,4]. Because of the trend of decreasing electronic device size, interest in functional Langmuir–Blodgett (LB) films has considerably developed in recent years [5,6]. LB films have been suggested as a route to the development of molecular dimension switches and storage

Address correspodence to Jian-Ming Ouyang, Institute of Biomineralization and Lithiasis Research, Jinan University, Guangzhou 510632, China. Tel. and Fax: 0086-20-85223353, E-mail: toyjm@jnu.edu.cn

elements used in energy conversion systems, sensors, and microscopic communication systems [7,8]. LB films containing metals or their ions have attracted much attention for constructing supramolecular catalytic systems and growing size-quantized semiconducers. The interaction between monolayers and metal ions in the subphase has been intensively investigated [9,10]. The functional groups of the monolayer-forming materials include dithiocarbamate, 8-hydroxyquinoline, imidazole, crown ethers, cyclam, and so forth. Compared with standard sensor technology, an LB film sensor has the advantages that an extremely small quantity of metal ion can be detected and an ordered molecule structure oriented especially to optimize complexation can be achieved [11,12].

With these in mind, we have synthesized a series of amphiphilic 8-aminoquinoline ligands, N,N′ -bis(8-quinolinyl) alkylpropanediamide (H_2A) [alkyl: dodecyl(H_2A^{12})and hexadecyl(H_2A^{16})]. The monolayer behavior of H_2A at the air–water interface was investigated. The interaction between the monolayer and many metal ions such as Mg^{2+}, Ca^{2+}, Mn^{2+}, Co^{2+}, Ni^{2+}, Cu^{2+}, Zn^{2+}, Cd^{2+}, Pb^{2+}, Hg^{2+}, and La^{3+} in the subphase was studied. The LB films of H_2A can detect the concentration of Cu(II) ion in the region of $1.0\times10^{-7} \sim 1.0 \times 1.0^{-6}$mol dm^{-3}.

EXPERIMENTAL

Materials

8-Aminoquinoline, 1-bromododecane, 1-bromohexadecane, and diethylmalonate were obtained from Sigma and Fluka. The metal salts such as $CaCl_2$, $MgCl_2$, $MnCl_2{\cdot}4H_2O$, $CoCl_2{\cdot}6H_2O$, $NiCl_2{\cdot}6H_2O$, $CuCl_2{\cdot}2H_2O$, $ZnCl_2$, $CdCl_2{\cdot}2.5H_2O$, $HgCl_2$, $PbCl_2$, and $LaCl_3{\cdot}7H_2O$ and all other chemicals were of analytical reagent (A.R) grade, purchased from Shanghai Chemical Reagents Co. Chloroform was purified by standard procedure. Water was purified with a Millipore Milli-Q system, obtaining a specific resistance of 18.2 MΩ·cm. The concentration of the metal ion in subphase was $1.0 \times 10^{-3}\,\mathrm{mol \cdot dm^{-3}}$. The pH of the aqueous subphase in equilibrium with air/CO_2 was approximately 5.6.

Synthesis of Amphiphilic Ligand H_2A

The synthesis procedure for the amphiphilic ligand, N,N′ -bis (8-quinolinyl) alkylpropane diamide (H_2A) is illustrated in Scheme 1. This route involved the preparation of α -alkyldiethylmalonate (**2**) and subsequent reaction with 8-aminoquinoline.

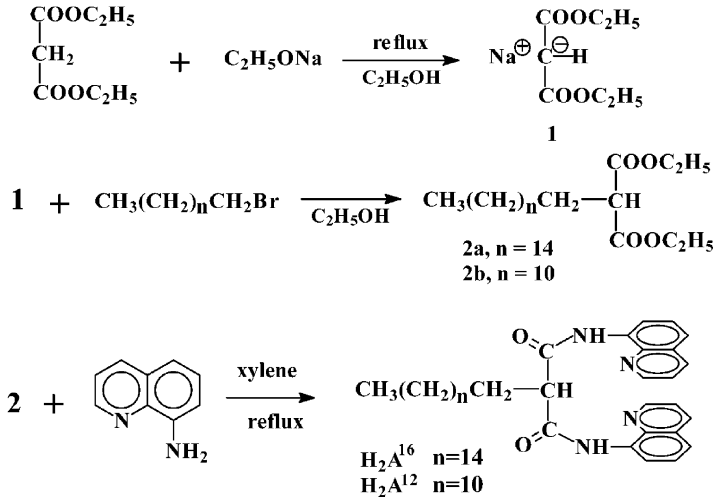

SCHEME 1 Synthesis of the amphiphilic ligands H_2A.

Syntheses of α-Hexadecyldiethylmalonate (2a) and α-Dodecyldiethylmalonate (2b)

Diethyl malonate (10.0 mmol, 1.52 ml) was added slowly into a 100-ml round-bottom, two-neck flask equipped with reflux condenser. The flask contained 10.5 mmol of new prepared ethanolic sodium in 15.0 ml ethanol. After the addition was complete, the reaction mixture was allowed to reflux for 15 h with stirring. A deep brown mixture (**1**) was obtained. Then, 10.5 mmol (2.52 ml) 1-bromohexadecane in 15.0 ml ethanol was added to the above solution. Reflux was continued for 15 hr. The product α-hexadecyl diethylmalonate **(2a)** was obtained by distillation. FT-IR ν_{max} (KBr): 2930, 2860 (CH_2, CH_3), 1735 (COOR), 1470 (CH_2), 1370 (CH_3), 1125, 1100, 1030, 861, 720 [$(CH_2)_n$] cm^{-1}. ^1H NMR ($CDCl_3$, TMS) δ_H: 4.22–4.11 (4H, $COOCH_2$), 3.98 (1 H, ≡CH), 2.31–2.30 (2H, CH_2), 1.34–1.26 (6H, $2CH_3$), 1.24–1.21 (28H, CH_2), 0.89–0.87 (3H, CH_3).

α-Dodecyldiethylmalonate **(2b)** was synthesized following the procedure of **2a**. FT-IR ν_{max} (KBr): 2926, 2859 (CH_2, CH_3), 1732 (COOR), 1467 (CH_2), 1369 (CH_3), 1223, 1100, 1033, 861, 722 [$(CH_2)_n$] cm^{-1}.

Synthesis of N,N′-Bis(8-Quinolinyl)Hexadecylpropanediamide (H_2A^{16})

The amphiphilic ligand, N,N′-bis(8-quinolinyl)hexadecylpropanediamide (H_2A^{16}), was synthesized by reaction of 8-aminoquinoline

(0.47 g, 3.3 mmol) with **2a** (0.58 g, 1.5 mmol) in freshly distilled xylene (20 ml). The mixture was refluxed for 10 h more. After the solvent was removed, the residue was recrystallized triple from hot petroleum ether (60–90°C) (animal charcoal). The product H_2A^{16} is a light grey powder. The yield was 50%. Mp 64–65°C. Elemental analysis: Found: C, 76.60; H, 8.54; N, 9.51%. Calcd. for $C_{37}H_{48}N_4O_2$: C, 76.55; H, 8.28; N, 9.66%. FAB-MS: 580 (M). FT-IR ν_{max} (KBr): 3290 (CONHAr), 2920, 2850 (CH_2, CH_3), 1671 (CONH), 1530, 1485, 1420, 1325 (phenyl ring), 830, 795, 760, 721.4 (CH_2) cm^{-1}; UV-Vis λ_{max} (log ε, in CH_3CH_2OH): 240.8 (4.70), 319 nm (4.30 L cm^{-1} mol^{-1}). ^1H NMR ($CDCl_3$, TMS) δ_H: 10.90 (1.44 H, Ar-NHR), 8.95–8.88 (2 H, Ar-H), 8.87–8.81 (2 H, Ar-H), 8.31–8.28 (2 H, Ar-H), 7.63–7.53 (6 H, Ar-H), 3.97–3.92 (1 H, ≡CH), 2.31–2.22 (2 H, CH_2), 1.86–1.51 (2 H, CH_2), 1.41–1.34 (2 H, CH_2), 1.23–1.19 (24 H, CH_2), 0.88–0.84 (3 H, CH_3).

Synthesis of N,N-Bis(8-Quinolinyl)Dodecylpropanediamide (H_2A^{12})

H_2A^{12} was synthesized by reaction of 8-aminoquinoline (0.47 g, 3.3 mmol) with **2b** (0.49 g, 1.5 mmol) following the procedure of H_2A^{16}. The product H_2A^{12} is also a light grey powder. The yield was 45%. Mp 56–57°C. Elemental analysis: Found: C, 75.15; H, 7.83; N, 10.20%. Calc. for $C_{33}H_{40}N_4O_2$: C, 75.57; H, 7.63; N, 10.69%. FAB-MS: 524 (M). FT-IR ν_{max} (KBr): 3282 (CONHAr), 2954, 2845 (CH_2, CH_3), 1664 (CONH), 1533, 1497, 1424, 1330 (phenyl ring), 826, 796, 756, 723 (CH_2) cm^{-1}. UV-Vis λ_{max} (log ε, in CH_3CH_2OH): 240.6 (4.72), 317.8 nm (4.15 L cm^{-1} mol^{-1}). ^1H NMR ($CDCl_3$, TMS) δ_H: 10.75 (1.4 H, Ar-NH_2), 8.91–8.90 (2 H, Ar-H), 8.86–8.84 (2 H, Ar-H), 8.19–8.14 (2 H, Ar-H), 7.57–7.52 (4 H, Ar-H), 7.49–7.47 (2 H, Ar-H), 3.75–3.74 (1 H, ≡CH), 2.30–2.26 (2 H, CH_2), 1.58–1.52 (2 H, CH_2), 1.43–1.37 (2 H, CH_2), 1.27–1.20 (16 H, CH_2), 0.88–0.85 (3 H, CH_3).

Formation of the Monolayer of H_2A and Deposition of the Langmuir–Blodgett Film

The solution of H_2A (1.0×10^{-3} mol dm^{-3} in chloroform) was applied dropwise to a clean subphase surface by a microsyringe. After the chloroform had evaporated (approx. 20 min), the monolayer was compressed at a rate of approximately 0.03 nm^2 $molecule^{-1}$ min^{-1}, and the isotherm of surface pressure (π) versus area per molecule (A) was recorded. The pH values of the subphases were adjusted by addition of isopiestically distilled HCl or NaOH solution; ,no buffer was used. NaCl was used to adjust the ionic strength in subphases. The pH of the aqueous subphase in equilibrium with air/CO_2 was

approximately 5.6. The π-A isotherms were reproducible and each experiment was repeated until three coincident curves were obtained.

The monolayers were transferred onto a hydrophilic quartz substrate at a constant surface pressure by the vertical dipping method. The transfer ratios of these LB films are about 1.00 ± 0.05 and 0.90 ± 0.05 for the down- and upstrokes, respectively. This indicates that the LB films were head-to-head bilayer films. The dipping speed was 3.0 mm min^{-1} for both the upstrokes and downstrokes. The quartz slides were washed in detergent and sonicated in a bath sonicator (ultrasonic cleaner). After the quartz slides were washed in deionized water, they were cleaned by heating (70°C) in a mixture of 30% H_2O_2 and concentrated H_2SO_4 (30:70 v/v) for 30 min [10]. The hydrophilic substrates were prepared by sonicating the substrates in 1.0 mol dm^{-3} NaOH for 5 min. After they were thoroughly rinsed with deionized water, the quartz slides were stored under water.

All work was carried out in a dust-free box at 25 ± 1°C.

Apparatus

Elemental analyses were prepared using a ST-02 Model elemental analyser. ^{1}H NMR spectra were obtained using a Bruker Am-500 NMR spectrometer with tetramethylsilane as an internal reference. FT-IR spectra were recorded on a Nicolet Model 170 SX FTIR spectrometer. Electronic spectra were measured with a Shimadzu Model 3100 UV-VIS-NIR recording spectrophotometer. Measurement of π-A isotherms was carried out with a British NIMA 2000 round trough. Low-angle X-ray diffraction results were recorded on a D/max-γA X-ray diffractometer (Japan), using Ni-filtered Cu-K_α radiation. The divergence and scattering slit was at l° for $1° < 2\theta < 8°$.

The analysis of X-ray photoelectron spectroscopy (XPS) was performed using an ESCALAB Mark II (VG) photoelectron spectrometer, with an Al K_α X-ray radiation source (1486.6 eV) under a vacuum of 10^{-7} Pa. A two-step procedure was used in these studies [13]. At first, wide spectra of the LB films were recorded. Careful examination of the spectra allows us to assign the observed peaks to particular components. In the second step the most characteristic peaks were recorded in narrow ranges of binding energy to obtain a better statistic and resolution required for an optimal spectral manipulation.

The spectra were analyzed and deconvoluted using the Vision Software. For the atomic-concentration calculation, the intensity of each peak was estimated from integration after having smoothed and subtracted a Shirlay-shaped background. Contributions for the spectra coming from the X-ray source satellites were also subtracted.

Overlapping signals were analyzed using a deconvolution into Gaussian/Lorenzian-shaped components.

RESULTS AND DISCUSSION

Monolayer Behavior of H_2A on Subphases with Different pH

Because H_2A^{16} and H_2A^{12} have similar structures, they are expected to have similar monolayer-forming properties. Therefore, only H_2A^{16} was investigated in detail.

The π-A isotherms of H_2A^{16} on a pure water surface (pH 5.6) and the aqueous subphases with different pH values are shown in Figure 1. These isotherms are similar. The state of the monolayer at air–water is expanded. The collapse pressures (π_{max}) of H_2A^{16} monolayers are about 15.5 mN m^{-1}. The areas per H_2A^{16} molecule at 10 mN m^{-1} (A_{10}) are about 0.85–0.90 nm^2. This indicates that little change in monolayer structure takes place and the likeness in the arrangement of the head groups in H_2A^{16} monolayers in a wide range of pH (2.0–11.0) [14]. However, the isotherms of H_2A^{16} on stronger basic subphases such as pH > 11.0 expand more than that on neutral and acidic subphases.

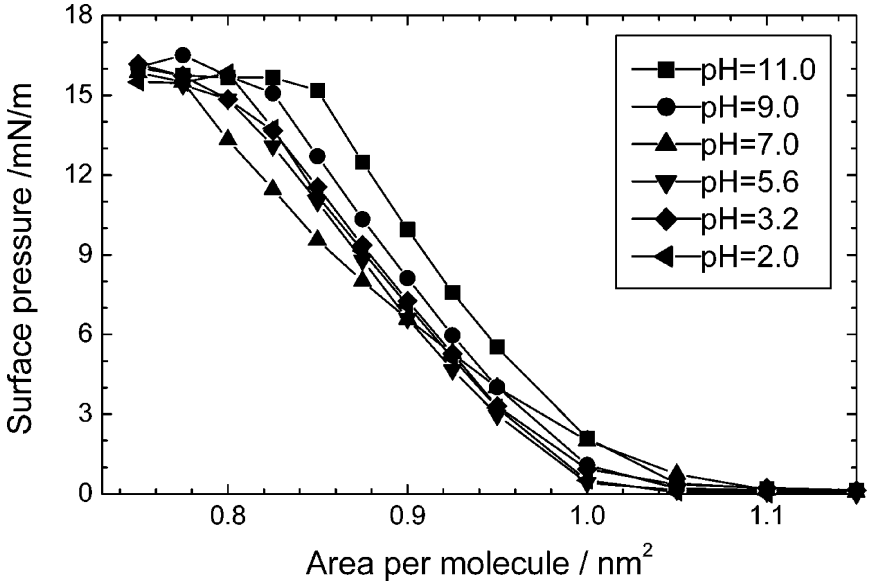

FIGURE 1 π-A isotherms of H_2A^{16} monolayer on subphases with various pH values at 25°C.

Effect of Metal Ions on H_2A Monolayer

In general, the molecular organization of the monolayer depends strongly on the composition of the subphase. The metal ions contained in subphases have a marked effect on the monolayer behavior, especially for monolayers of amphiphilic molecules with coordinating head group. Therefore, the monolayer film of H_2A^{16} is expected to be manifested by the metal ions present in the subphases. It was very interesting that many metal ions, such as the main group metallic ions Mg^{2+}, Ca^{2+}, and Pb^{2+} and the transitional metallic ions Mn^{2+}, Co^{2+}, Ni^{2+}, Zn^{2+}, Cd^{2+}, Hg^{2+}, and La^{3+}, contained in subphases showed little or no influence on the π-A isotherms of the H_2A^{16} monolayers. Only the Cu^{2+} ion has special modification on H_2A^{16} monolayers. The areas per H_2A^{16} molecule at 10 mN m^{-1} (A_{10}) and the collapse pressures of the H_2A^{16} monolayers on subphases containing various metal ions are shown in Table 1.

When 1.0×10^{-3} mol dm^{-3} $CuCl_2$ is added in the subphase, the collapse pressure of the H_2A^{16} monolayer increases to 33.8 mN m^{-1} from approximately 15.5 mN m^{-1} on pure water subphase. The area per molecule H_2A^{16} at 10 mN m^{-1} increases to 1.05 nm^2 from approximately 0.84 nm^2. The pronounced difference seen with copper could be due to monomeric complex formation, or it could be due to linking molecules to form dimmers. This indicates that Cu^{2+} ions can coordinate with H_2A^{16} at the air–water interface. This coordination was verified by X-ray photoelectron spectroscopy and will be discussed in detail in next section. This special coordination of H_2A^{16} with Cu^{2+} ion may be developed as a Cu^{2+} ion sensor.

The concentration of $CuCl_2$ on subphase has an apparent effect on the isotherms. Figure 2 shows the π-A isotherms of H_2A^{16} monolayers on subphases containing different concentrations of $CuCl_2$. The isotherms of H_2A^{16} on subphases containing 5.0×10^{-8} or 1.0×10^{-7} mol dm^{-3} $CuCl_2$ were nearly the same as that of H_2A^{16} on pure water

TABLE 1 Collapse Pressure (π_{max}) and the Area per H_2A^{16} Molecule at 10 mN m^{-1} (A_{10}) on Subphases Containing Different Metal Ions ($[MCl_2] = 1.0$ mmol dm^{-3})

Metal salt	H_2O	$CuCl_2$	$MgCl_2$	$CaCl_2$	$MnCl_2$	$CoCl_2$	$NiCl_2$	$ZnCl_2$	$CdCl_2$	$PbCl_2$	$HgCl_2$	$LaCl_3$
π_{max} (mN m^{-1})	15.5	33.8	15.8	16.0	15.6	15.7	16.0	16.2	15.4	15.9	15.6	16.3
A_{10} (nm^2)	0.84	1.05	0.83	0.87	0.86	0.89	0.86	0.85	0.87	0.85	0.86	0.86

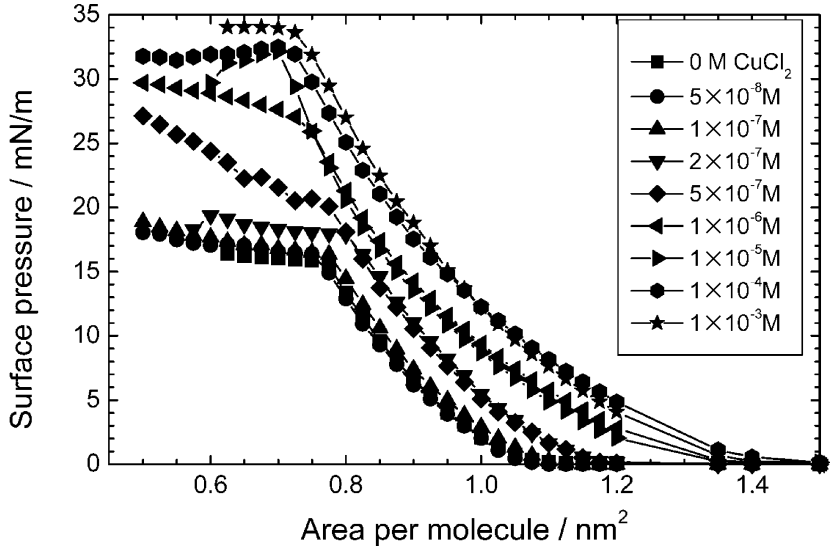

FIGURE 2 π-A isotherms of H_2A^{16} on subphases containing different concentrations of $CuCl_2$; pH = 5.6.

subphase. It suggests that no complexation of H_2A^{16} with Cu^{2+} ions took place at the air-water interface under this condition. When the concentration of $CuCl_2$ increased to 3.0×10^{-6} mol dm^{-3}, the π-A isotherm showed very different characteristics. The collapse pressure increased to 32.5 mN m^{-1}. When the concentration of $CuCl_2$ in the subphase was larger than 3.0×10^{-6} mol dm^{-3}, the π-A isotherms showed little change.

However, in the concentration range from 1.0×10^{-7} to 3.0×10^{-6} mol dm^{-3} $CuCl_2$, both the collapse pressures and the features of H_2A^{16} monolayers changed markedly, depending on the concentration of $CuCl_2$. It suggests that H_2A^{16} may detect the concentration of copper ion in the range from 1.0×10^{-7} to 3.0×10^{-6} mol dm^{-3}.

The π-A isotherms of H_2A^{12} monolayers were similar to those of H_2A^{16}, as shown in Figure 3. However, the isotherms of H_2A^{12} monolayer showed a little shift to a smaller molecular area with a decrease of the collapse pressure in comparison with that of H_2A^{16}.

XPS of Metal–H_2A LB Films

X-ray photoelectron spectroscopy (XPS) was utilized to investigate the uppermost layers of a solid, including a probing depth of approximately

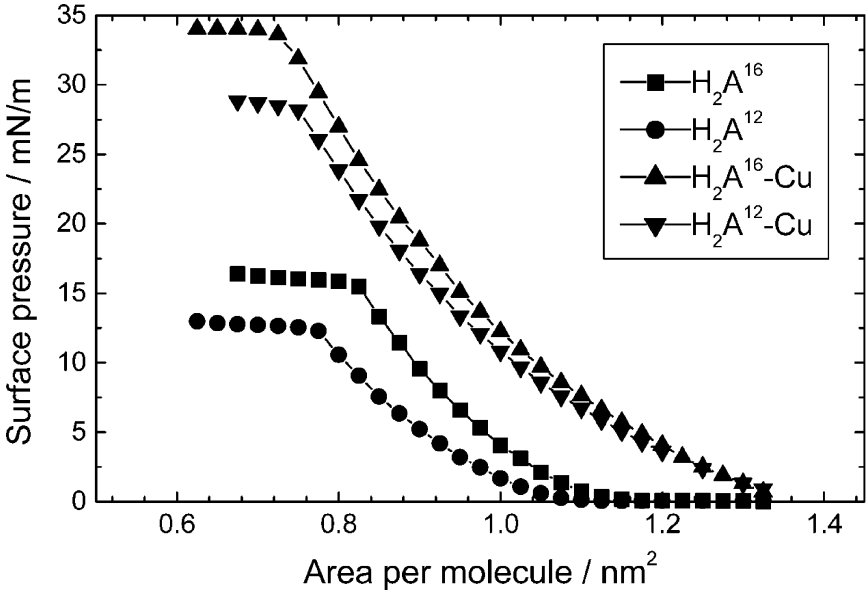

FIGURE 3 π-A isotherms of H_2A^{16} and H_2A^{12} on subphases with and without Cu^{2+} ion; pH = 5.6.

1.0–10.0 nm, depending on the property of materials probed. This depth is just the thickness of about one to several layers of LB films. To investigate further the complexation of amphiphilic ligand H_2A with Cu^{2+} or other ions containing subphase and any special characteristics of metal–H_2A binding, elemental analyses of built-up LB film of H_2A^{16}, deposited from subphases with Cu^{2+}, Co^{2+}, or Ni^{2+} ions, were performed by means of XPS measurements.

The XPS spectrum of a two-layer LB film of H_2A^{16} built up from a 1.0×10^{-3} mol dm^{-3} $CuCl_2$ subphase is shown in Figure 4. We can clearly see the copper peaks (933.25 and 953.3 eV) in the XPS spectrum (the insert in Fig. 4). That is, a complexation of H_2A^{16} with Cu^{2+} ion took place at the air–water interface and the complex (Cu-H_2A^{16}) monolayers were transferred onto quartz plate. However, there is nearly no Co or Ni peaks in the XPS spectra of H_2A^{16} LB films built up from a 1.0×10^{-3} mol dm^{-3} $CoCl_2$ or $NiCl_2$ subphase. It indicated that H_2A^{16} cannot complex with Co^{2+}, Ni^{2+} ions at the air–water interface.

Binding energy (E_b) in XPS spectrum depends on a small but measurable chemical shift resulting from the atomic charges localized both on the ionized and on the neighboring atoms and is therefore

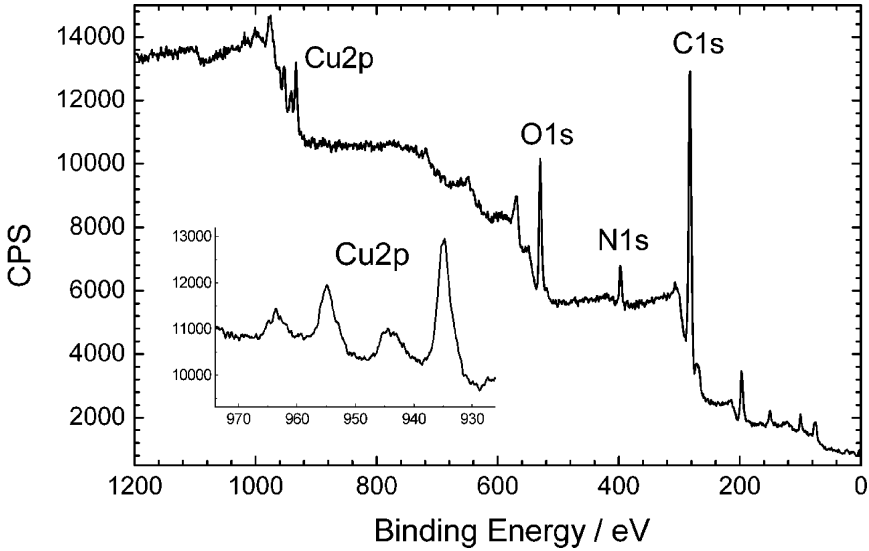

FIGURE 4 XPS spectra for a two-layer LB film of H_2A^{16} transferred from a 1.0×10^{-3} mol dm^{-3} $CuCl_2$ subphase. The insert shows the absorption peak of Cu2p.

related to the net atomic charges. Because the factors that affect the measured XPS binding energy depend on the nature of the chemical surroundings, a direct experimental characterization of such important quantities as the energy of molecular orbital levels and atomic charge distributions within the coordination sphere is available.

Compared with the binding energy of N1 s (399.80 and 399.85 eV) in $H_2A^{16}$and H_2A^{12} LB film, which increased to 400.5 and 400.25 eV in Cu-H_2A^{16} and Cu-H_2A^{12} LB films, respectively. It is clear that the lone pair electrons from the nitrogen atoms were shifted into the copper atom and thereby a strong complexation was formed. That is, $H_2A^{16}$and H_2A^{12} were coordinated to Cu^{2+} ion in subphase through the amide N atoms and the heterocyclic N atoms. However, the binding energy of O1 s (approx. 529.9 eV) showed little change. It indicated the oxygen atoms in CONHAr groups did not coordinate with Cu^{2+} ion. The charge transfer from N atoms of H_2A to Cu^{2+} ion led to a decrease of charge density and an increase of binding energy of N atoms.

The information on stoichiometry provided by XPS gave the elemental C/Cu ratios of Cu-H_2A^{16} and Cu-H_2A^{12} LB films (estimated from the relative signal strength of the XPS peaks) to be 35.4 and 32.0,

which is consistent with the theoretical C/Cu ratio of 37.0 and 33.0. This shows that a copper ion is coordinated by one H_2A^{16} or H_2A^{12} molecule. That is, H_2A is deposited as a complex (Cu-H_2A) from the $CuCl_2$ subsolution. The 1:1 coordination ratio of H_2A with Cu^{2+} ion at the monolayer/water interface is the same as that in bulk solutions. In acetone, for example, a 1:1 complex (CuA^{16} and CuA^{12}) was also obtained.

UV-vis Spectra of H_2A LB Films

The UV-vis spectroscopy of the monolayer at the air–water interface provides useful information on the interactions. The UV-vis spectra of H_2A^{16} LB films deposited from pure water subphase and subphase containing 1.0×10^{-3} mol dm^{-3} $CuCl_2$ or $NiCl_2$ or $CoCl_2$ were measured. On pure water subsolution, the LB film of H_2A^{16} shows two absorption peaks at 246 and 324 nm, as shown in Figure 5c. However, the principal peak at 324 nm disappeared and a new peak maximum at approximately. 395 and 396 nm was observed, respectively, for H_2A^{16} (Fig. 5a) and H_2A^{12} LB films (Fig. 5b) deposited from $CuCl_2$ subsolution. These new bands are assigned to an electron-transfer transition from the nitrogen atoms in the quinoline ring to the hole in the 3d

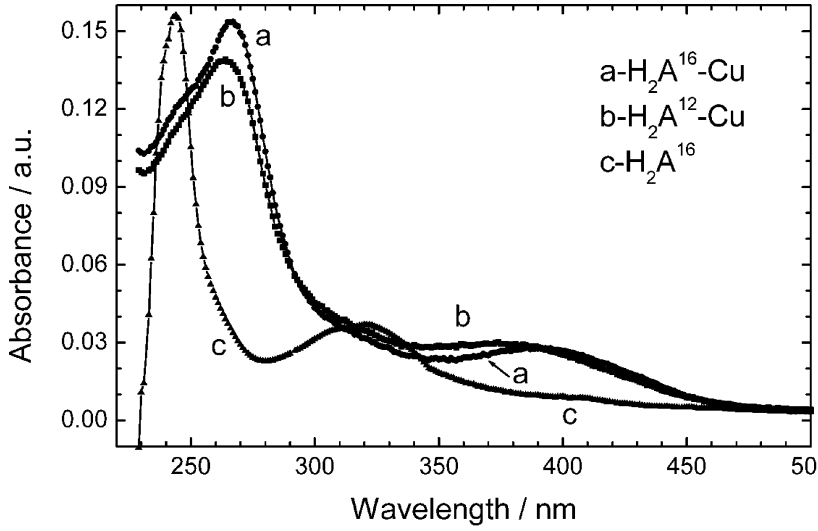

FIGURE 5 UV-vis spectra of the monolayers of H_2A^{16} and H_2A^{12} on subphase containing 1.0×10^{-3} mol dm^{-3} $CuCl_2$, and the monolayer of H_2A^{16} on pure water subphase.

shell of Cu^{2+} ion [15,16]. This result further shows the formation of a complex between H_2A and Cu^{2+} ion.

However, when the other metal ions such as Co^{2+} or Ni^{2+} ions were added in the subphases, the UV-vis spectra of H_2A^{16} LB films deposited from subphases containing these ions have no this new peak maximum at approximately 395–400 nm. It indicates that there is no complexation between H^2A and Co^{2+} or Ni^{2+} ions.

Compared with the absorption of the H_2A^{16} in LB films and in ethanol solution, red shifts of about 5.2 nm at the 240.8 nm band (from 240.8 to 246 nm) and of about 5.0 nm at the 319 nm band (from 319 nm to 324 nm) were observed. This likely is due to crystallization effects and indicates that there is a strong interaction between the molecules of H_2A^{16} in the LB films.

Copper Ion Sensor

The above results led to the conclusion that H_2A formed complex with Cu^{2+} ion in the interfacial region, and that it was possible to utilize the LB film technique to fabricate a Cu^{2+} ion sensor.

First, one layer of arachidic acid was deposited onto a quartz substrate (upstroke, 25 mN m^{-1}), and then one layer of sensing moieties, H_2A^{16}, was transferred onto this substrate from pure water subphase (downstroke, 10 mN m^{-1}). After this procedure, the complexing 8-aminoquinoline groups of H_2A^{16} are oriented outward in the LB film. After immersing the LB film in 5.0×10^{-8}, 1.0×10^{-7}, 2.0×10^{-7}, 5.0×10^{-7}, 1.0×10^{-6}, 2.0×10^{-6}, and 4.0×10^{-6} mol dm^{-3} $CuCl_2$ for 15 min, the solutions were exchanged against redistilled water and the UV-vis spectra were recorded in Figure 6.

The UV-vis spectra of the LB films of H_2A^{16} after immersing in Cu^{2+} ion solution (Fig. 6) were similar to those of the LB films of H_2A^{16} deposited from $CuCl_2$ subsolution (Fig. 5a). This shows that the Cu^{2+} ions in aqueous solution have formed complexes with the H_2A^{16} molecules in the LB films. The absorbance of the H_2A^{16} LB films depended on the concentrations of $CuCl_2$ in the range from 1.0×10^{-7} to 1.0×10^{-6} mol dm^{-3} (Figure 7). That is, the H_2A^{16} LB film transferred from the pure water subphase can identify whether there are Cu^{2+} ions in the solution and, furthermore, can detect the concentration of Cu^{2+} ions in the region of $1.0 \times 10^{-7} \sim 1.0 \times 10^{-6}$ mol dm^{-3}.

CONCLUSION

Two amphiphilic ligands based on 8-aminoquinoline, H_2A^{12} and H_2A^{16}, were synthesized and characterized by FT-IR, ^1H NMR, and

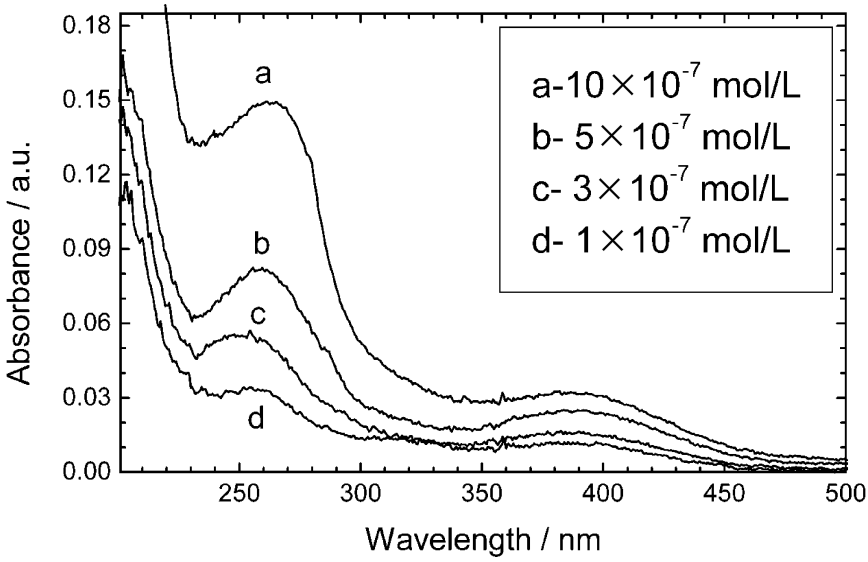

FIGURE 6 UV-vis spectra of H_2A^{16} LB films after immersion in different concentrations of $CuCl_2$ solution.

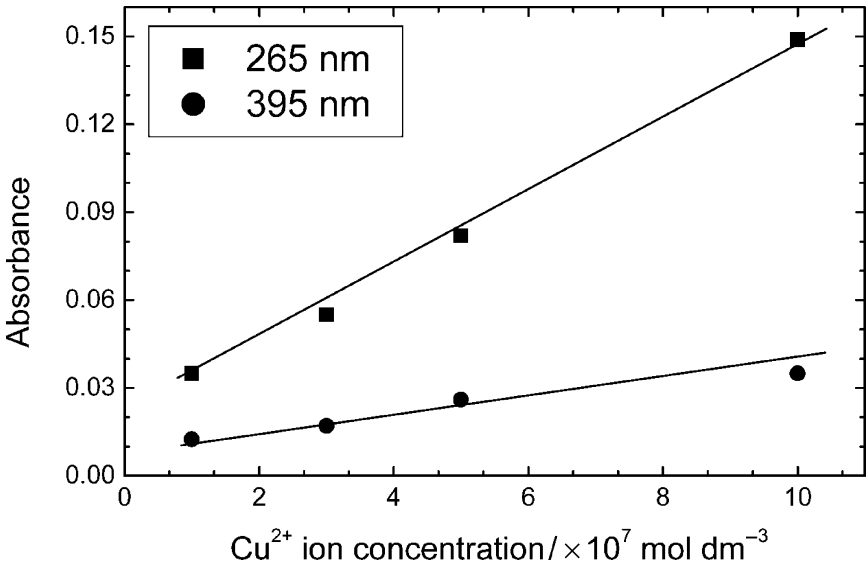

FIGURE 7 The dependence of the absorbance of Cu-H_2A^{16} LB films on concentrations of $CuCl_2$ solution.

UV-vis spectroscopy. H_2A can form stable monolayers. The pH values in subphases show little effect on the behavior of H_2A monolayers in a wide range of 2.0–11.0. Only the Cu^{2+} ion has special coordination with H_2A monolayers. The other metallic ions such as Mg^{2+}, Ca^{2+}, Pb^{2+}, Mn^{2+}, Co^{2+}, Ni^{2+}, Cu^{2+}, Zn^{2+}, Cd^{2+}, Hg^{2+}, and La^{3+} show no interaction with H_2A monolayer. The collapse pressures of H_2A^{16} and H_2A^{12} monolayers are 12 and 15.5 mN m^{-1} on pure water subphase, respectively, and increase to 27.5 and 33.8 mN m^{-1} after coordination with Cu^{2+} ions. XPS spectra show the presence of the copper peaks at 933.25 and 953.3 eV. The information on stoichiometry provided by XPS shows a copper ion is coordinated by one H_2A^{16} or H_2A^{12} molecule. The H_2A^{16} LB film transferred from pure water subphase can identify whether there are Cu^{2+} ions in the solution and, furthermore, can detect the concentration of Cu^{2+} ions in the region of $1.0 \times 10^{-7} \sim 1.0 \times 10^{-6}$ mol dm^{-3}.

ACKNOWLEDGMENTS

This research work was supported by the Natural Science Foundation of China, the Key Project of Natural Science Foundation of Guangdong Province (Grant Nos. 2001C31401 and 013202), and Foundation of State Key Laboratory of Materials Chemisrty and Applications of Peking University of China.

REFERENCES

[1] Zheng, Y., Orbulescu, J., Ji, X., Andreopoulos, F. M., Pham, S. M., & Leblanc, R. M. (2003). *J. Am. Chem. Soc.*, *125*(9), 2680–2686.
[2] Kent, M. S., Yim, H., Sasaki, D. Y., Majewski, J., Smith, G. S., Shin, K., Satija, S., & Ocko, B. M. (2002). *Langmuir*, *18*(9), 3754–3757.
[3] Ouyang, J.-M., Xue, P., & Ngan, H.-I. (2001). *Chem. Lett.*, *30*(2), 104–105.
[4] Chen, H.-J., Xu, J.-F., & Li, Z.-L. (1998). *J. Chem. Res.*, 444–445.
[5] Ouyang, J.-M. (1999). *Princical and application of Langmuir–Blodgett*, Guangzou: Jinan University Press, Chapter 5.
[6] Riul, A., Gallardo Soto, A. M., Mello, S. V., Bone, S., Taylor, D. M., & Mattoso, L. H. C. (2003). *Synth. Metals*, *132*(2), 109–116.
[7] Matsui, J., Mitsuishi, M., Aoki, A., & Miyashita, T. (2003). *Angew. Chem., Int. Ed. Engl.*, *42*(20), 2272–2275.
[8] Paul, S., Pearson, C., Molloy, A., Cousins, M. A., Green, M., Kolliopoulou, S., Dimitrakis, P., Normand, P., Tsoukalas, D., & Petty, M. C. (2003). *Nano Lett.*, *3*(4), 533–536.
[9] Ng, S. C., Zhou, X. C., Chen, Z. K., Miao, P., Chan, H. S. O., Li, S. F. Y., & Fu, P. (1998). *Langmuir*, *14*(7), 1748–1752.
[10] Ouyang, J.-M., Li, C., & Li, Y.-Q. (1999). *Thin Solid Films*, *348*, 242–247.
[11] Ferreira, M., Riul, A. Jr., Wohnrath, K., Fonseca, F. J., Oliveira, O. N. Jr., & Mattoso, L. H. C. (2003). *Anal. Chem.*, *75*(4), 953–955.

[12] Kalinina, M. A., Arslanov, V. V., & Vatsadze, S. Z. (2003). *Coll. J.*, *65*(2), 177–185.
[13] Ouyang, J.-M., Zheng, W.-J., Huang, N.-X., & Tai, Z.-H. (1999). *Thin Solid Films*, *340*, 257–262.
[14] Ouyang, J.-M., Zheng, W.-J., & Li, C. (1999). *Mater. Sci. Eng. C*, *10*, 115–118.
[15] Ouyang, J.-M., Tai, Z.-H., & Tang, W.-X. (1996). *Thin Solid Films*, *289*, 199–204.
[16] Budach, W., Ahuja, R. C., & Moebius, D. (1993). *Langmuir*, *9*(11), 3093–3100.